

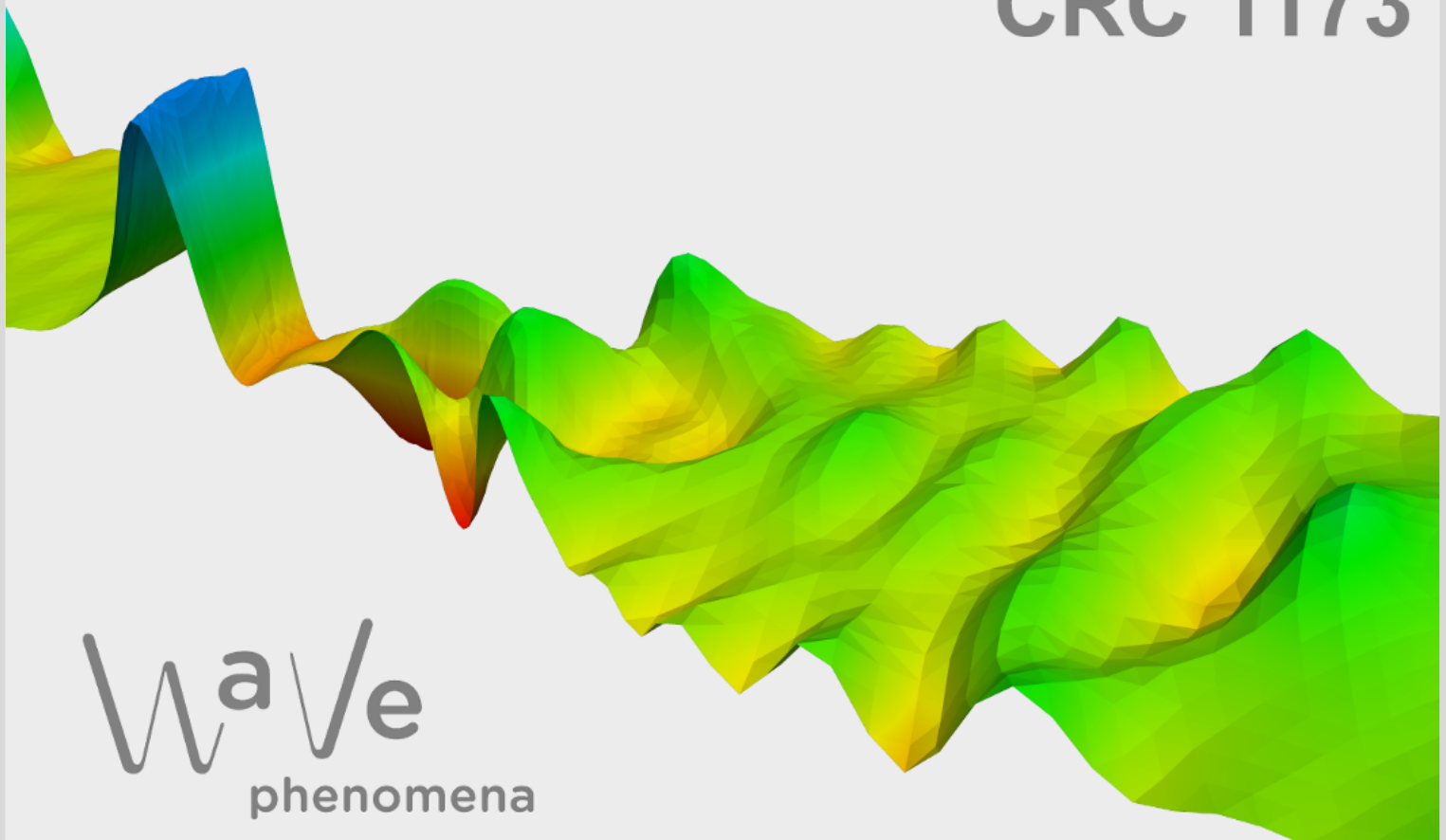
Microlocal analysis of imaging operators for effective common offset seismic reconstruction

Christine Grathwohl, Peer Kunstmann,
Andreas Rieder Eric Todd Quinto

CRC Preprint 2018/9, June 2018

KARLSRUHE INSTITUTE OF TECHNOLOGY

CRC 1173



Wave
phenomena

Participating universities



Universität Stuttgart

EBERHARD KARLS
UNIVERSITÄT
TÜBINGEN



Funded by

DFG

ISSN 2365-662X

MICROLOCAL ANALYSIS OF IMAGING OPERATORS FOR EFFECTIVE COMMON OFFSET SEISMIC RECONSTRUCTION

CHRISTINE GRATHWOHL, PEER KUNSTMANN, ERIC TODD QUINTO,
AND ANDREAS RIEDER

ABSTRACT. The elliptic Radon transform (eRT) integrates functions over ellipses in 2D and ellipsoids of revolution in 3D. It thus serves as a model for linearized seismic imaging under the common offset scanning geometry where sources and receivers are offset by a constant vector. As an inversion formula of eRT is unknown we propose certain imaging operators (generalized backprojection operators) which allow to reconstruct some singularities of the searched-for function from seismic measurements. We calculate and analyze the top order symbols of these imaging operators as pseudo-differential operators to understand how they map, emphasize or de-emphasize singularities. We use this information to develop local reconstruction operators that reconstruct relatively independently of depth and offset. Numerical examples illustrate the theoretical findings.

1. INTRODUCTION

In seismic imaging one penetrates the earth's subsurface with pressure waves which are generated on the surface. The geological inner structure scatters the waves and those parts returning to the surface are picked up by receivers. The corresponding inverse problem entails imaging the subsurface from these scattered waves. For a first quick reconstruction in the acoustic regime linearized models are used, for instance, classical Kirchhoff migration.

Traditional Kirchhoff migration may mathematically be described by

$$f_{\text{recon}} = F^\# P g \quad \text{where } g = F f \text{ are the data (measurements).}$$

The operator F above is a generalized Radon transform, P is a one-dimensional convolution operator and $F^\#$ is a kind of dual transform (generalized backprojection). Beylkin [1] showed for a specific $F^\#$ that

$$f_{\text{recon}} = F^\# P F f = I_{\text{partial}} f + \Psi f$$

where I_{partial} is a kind of band pass filter (operator of partial reconstruction) and Ψ is smoothing. Note that $F^\# P F$ is a pseudodifferential operator (Ψ DO) of non-negative order.

As we cannot hope to recover f from the data completely we consider imaging operators which differ from the Kirchhoff operator $F^\# P F$. Our operators are, in

Date: June 1, 2018.

2010 Mathematics Subject Classification. 58J40, 57R45, 86A15, 86A22, 35S30.

Key words and phrases. Generalized Radon transforms, Fourier integral operators, Microlocal analysis, Seismic imaging.

We gratefully acknowledge financial support by the Deutsche Forschungsgemeinschaft through CRC 1173. Quinto's work was partially supported by U.S. NSF grants DMS 1311558 and DMS 1712207 as well as funds from the Tufts University Faculty Research Awards Committee. The authors received no financial benefit from this work.

general, of the form

$$\Lambda = KF^\dagger\psi F$$

where ψ is a smooth cutoff function, F^\dagger is a weighted L^2 dual of F and K is a local operator such that Λ is of positive order so as to emphasize singularities.

In this article we restrict ourselves to a constant background velocity and to the common offset scanning geometry where source and receiver positions differ by a constant vector. Then, F becomes the elliptic Radon transform which integrates functions over ellipses in 2D and prolate spheroids in 3D with source and receiver positions as foci. We will argue that Λ is a Ψ DO and we will compute its top order symbol.

We analyze the symbol for the 2D setting¹ microlocally and use this information to design local operators K leading to imaging operators Λ with favorable properties. For instance, let $F^\dagger = F^*$ (formal L^2 -adjoint without weight) and

$$(1.1) \quad K = \Delta M + \alpha \text{Id}$$

where $2\alpha \geq 0$ is the distance between source and receiver, Δ is the Laplacian differential operator, and M denotes the multiplication operator by the depth-coordinate.² Then, Λ yields an imaging operator of order 1 with the following meaningful property: Jumps in f having the same height but being located at different depths will be visible in Λf with the same intensities almost independent of α .³

The mapping properties of Λ for several choices of K will be illustrated by numerical reconstructions using our migration scheme developed in [14]. The present paper is a follow-up of [14] where we used $K = \Delta$. Indeed, it was initiated by our wish to understand certain features in the reconstructions we obtained, and we address these now.

Our main tool in this paper is microlocal analysis which has been used before very successfully to analyze operators not only in seismics but also in other imaging techniques. First to mention here is the paper [8] where Felea et al. compare $F^*\psi F$ under the common midpoint and the common offset acquisition geometries in 3D. While in the former geometry the imaging operator is a singular Fourier integral operator (FIO), in the latter geometry this operator becomes a Ψ DO. To this end the authors verify the Bolker assumption for the common offset geometry and this is the result we will rely on. Further, we heavily benefit from [26] where Quinto showed how to express the symbol of generalized Radon transforms in terms of defining measures.

Microlocal properties of F and $F^*\psi F$ in various geometric settings have been studied by many authors, see, e.g. [7, 10, 11, 15, 20, 24, 27, 28, 29]. This list is surely not complete. We should point out that work on the Dirichlet to Neumann map, such as [31], provides insight into the seismic problem by giving local and microlocal information about density of the earth from local measurements with arbitrary sources and receivers. Because this requires independent sources and receivers, it does not exactly correspond to our problem. Recovery of microlocal information from seismic data is described in articles such as [23, 32, 34, 33, 36, 37] and, for reverse time migration, in [3]. A Radon transform perspective using curvelets is provided in [6]. Finally, we like to refer to the lecture notes [35, Section 8] where Symes derived a rather implicit expression for the top order symbol of F^*F by formal arguments.

¹The 3D case is much more involved and will be published elsewhere.

²The notion 'depth' refers to the distance from each given point in the earth's interior to the surface.

³For this short explanation of the mapping properties of Λ , we neglect the influence of the cutoff ψ and of the microlocal ellipticity of Λ . These points will be discussed later in the article.

We have organized our material as follows. For a largely self-contained presentation we derive F in the next section from the acoustic wave equation in 3D by the Born ansatz. Here we basically follow [35] and [4]. Then, in Section 3, we formulate the top order symbol of Λ in 2D and 3D. All technical details of the corresponding proofs, however, are moved to the final Section 5. In Section 4 we discuss the consequences from the symbol calculation for a concrete imaging situation in 2D. Our choice (1.1) for the operator K will become evident and its influence on the reconstructed images will be highlighted by numerical examples.

2. THE FORWARD OPERATORS OF LINEAR SEISMIC IMAGING

Let $u(t; \mathbf{x}, \mathbf{x}_s)$ be the acoustic potential in $\mathbf{x} \in \mathbb{R}^3$ at time $t \geq 0$ satisfying the acoustic wave equation with constant mass density and sound speed $\nu = \nu(\mathbf{x})$:

$$(2.1) \quad \frac{1}{\nu^2} \partial_t^2 u - \Delta_{\mathbf{x}} u = \delta(\mathbf{x} - \mathbf{x}_s) \delta(t)$$

where \mathbf{x}_s denotes the source points. Further, before firing the energy source, we can reliably assume the environment to be at rest:

$$(2.2) \quad u(0; \cdot, \mathbf{x}_s) = \partial_t u(0; \cdot, \mathbf{x}_s) = 0.$$

We want to recover ν from measurements $u(t; \mathbf{x}_r, \mathbf{x}_s)$ where \mathbf{x}_r denotes the receiver positions and t ranges over an observation period.

We are making the *Born ansatz*

$$(2.3) \quad \frac{1}{\nu^2(\mathbf{x})} = \frac{1 + n(\mathbf{x})}{c^2(\mathbf{x})}$$

with a smooth and a priori known background velocity $c = c(\mathbf{x})$. The dimensionless quantity n is the object we seek. It captures the high frequency variations of ν , see, e.g., [2, Chap. 3.2.1]. We derive a linear integral equation for n . Based on [4] and [35], most of the following material has already been presented in [14] for the two dimensional setting, however.

Let \tilde{u} denote the solution of the above wave equation with sound speed c , i.e.,

$$(2.4) \quad \frac{1}{c^2} \partial_t^2 \tilde{u} - \Delta_{\mathbf{x}} \tilde{u} = \delta(\mathbf{x} - \mathbf{x}_s) \delta(t)$$

where u and \tilde{u} share the same initial data (2.2). We will use \tilde{u} to derive a linear equation for n .

Subtracting (2.1) from (2.4) and given (2.3) we find the equation

$$\frac{1}{c^2} \partial_t^2 (\tilde{u} - u) - \Delta_{\mathbf{x}} (\tilde{u} - u) = \frac{n}{c^2} \partial_t^2 u.$$

Replacing u by \tilde{u} on the right of the above equation we define the linear map

$$L: n \mapsto u_d|_Y$$

where Y is the set of receivers and u_d solves

$$(2.5) \quad \frac{1}{c^2} \partial_t^2 u_d - \Delta_{\mathbf{x}} u_d = \frac{n}{c^2} \partial_t^2 \tilde{u}$$

with zero initial data (2.2). Now the linearized inverse problem in seismic imaging reads: Determine n from

$$Ln = \tilde{u}|_Y - u|_Y$$

where $u|_Y$ has been recorded and $\tilde{u}|_Y$ has to be computed from (2.4).

A straightforward calculation shows that

$$(2.6) \quad Ln(t; \cdot, \mathbf{x}_s) = \int \frac{n(\mathbf{x})}{c^2(\mathbf{x})} \left(\int_0^t \partial_t^2 \tilde{u}(s; \mathbf{x}, \mathbf{x}_s) \tilde{u}(t-s; \cdot, \mathbf{x}) ds \right) d\mathbf{x}$$

solves (2.5) formally with homogeneous initial values. To proceed we rely on the single ray assumption (geometric optics approximation) that is, $\mathbf{x} \in \text{supp } n$ can be connected to each \mathbf{x}_r and to each \mathbf{x}_s by exactly one ray of geometric optics. Accordingly, \tilde{u} is a progressing wave in 3D (from here our presentation differs from [14] as a progressing wave in 2D is differently represented):

$$(2.7) \quad \tilde{u}(t; \mathbf{x}, \mathbf{x}_s) \approx a(\mathbf{x}, \mathbf{x}_s) \delta(t - \tau(\mathbf{x}, \mathbf{x}_s))$$

in which the travel time $\tau(\mathbf{x}, \mathbf{x}_s)$ solves the eikonal equation

$$|\nabla_{\mathbf{x}} \tau| = \frac{1}{c}$$

and the amplitude a satisfies

$$\text{div}(a^2 \nabla_{\mathbf{x}} \tau) = 0,$$

see, e.g., Symes [35, pp. 24-25]. See also Friedlander [9] and Courant and Hilbert [5].

Plugging (2.7) into (2.6),

$$\begin{aligned} Ln(t; \mathbf{x}_r, \mathbf{x}_s) &\approx \int \frac{n(\mathbf{x})}{c^2(\mathbf{x})} a(\mathbf{x}, \mathbf{x}_s) a(\mathbf{x}_r, \mathbf{x}) \left(\int_0^t \delta''(s - \tau(\mathbf{x}, \mathbf{x}_s)) \delta(t - s - \tau(\mathbf{x}_r, \mathbf{x})) ds \right) d\mathbf{x} \\ &= \int \frac{n(\mathbf{x})}{c^2(\mathbf{x})} a(\mathbf{x}, \mathbf{x}_s) a(\mathbf{x}_r, \mathbf{x}) \delta''(t - \tau(\mathbf{x}, \mathbf{x}_s) - \tau(\mathbf{x}_r, \mathbf{x})) d\mathbf{x} \\ &= \partial_t^2 \int \frac{n(\mathbf{x})}{c^2(\mathbf{x})} a(\mathbf{x}, \mathbf{x}_s) a(\mathbf{x}_r, \mathbf{x}) \delta(t - \tau(\mathbf{x}, \mathbf{x}_s) - \tau(\mathbf{x}, \mathbf{x}_r)) d\mathbf{x} =: \tilde{L}n(t; \mathbf{x}_r, \mathbf{x}_s) \end{aligned}$$

where the first equality holds provided no forward scattering occurs, i.e.,

$$\nabla_{\mathbf{x}} \tau(\mathbf{x}, \mathbf{x}_r) + \nabla_{\mathbf{x}} \tau(\mathbf{x}, \mathbf{x}_s) \neq 0.$$

Set $u_{\text{data}} := \tilde{u} - u$. Our intermediate linear problem now reads

$$\tilde{L}n(t; \mathbf{x}_r, \mathbf{x}_s) = u_{\text{data}}(t; \mathbf{x}_r, \mathbf{x}_s)$$

and integrating both sides twice with respect to t over the observation period from 0 to T we finally obtain

$$(2.8) \quad Fn(T; \mathbf{x}_r, \mathbf{x}_s) = y(T; \mathbf{x}_r, \mathbf{x}_s)$$

where

$$y(T; \mathbf{x}_r, \mathbf{x}_s) := \int_0^T (T-t) u_{\text{data}}(t; \mathbf{x}_r, \mathbf{x}_s) dt$$

and

$$(2.9) \quad Fn(T; \mathbf{x}_r, \mathbf{x}_s) = \int \frac{n(\mathbf{x})}{c^2(\mathbf{x})} a(\mathbf{x}, \mathbf{x}_s) a(\mathbf{x}_r, \mathbf{x}) \delta(T - \tau(\mathbf{x}, \mathbf{x}_s) - \tau(\mathbf{x}, \mathbf{x}_r)) d\mathbf{x}$$

is a generalized Radon transform which integrates over reflection isochrones $\{\mathbf{x} : T = \tau(\mathbf{x}, \mathbf{x}_s) + \tau(\mathbf{x}, \mathbf{x}_r)\}$. The forward operator in 2D looks exactly the same, however, the right hand sides y of (2.8) differ for 2D and 3D, see [14].

From now on we consider both spatial dimensions. Thus, let $d \in \{2, 3\}$. We further proceed under the following assumptions

- the background velocity c is constant, say, $c = 1$,

- $n \in L^2(X)$ is compactly supported in $X = \mathbb{R}_+^d$ which is the lower half space, that is, $x_d > 0$ (the positive direction of the x_d -axis points downwards to the interior of the earth),
- as raw seismic data can be synthesized to provide common offset data [30, p. 59], we position sources and receivers according to the *common offset data acquisition geometry* on the hyperplane $x_d = 0$. Let $\alpha \geq 0$ be the common offset. Then, sources and receivers are parameterized by $s \in \mathbb{R}$ ($d = 2$) and $\mathbf{s} \in \mathbb{R}^2$ ($d = 3$) via

$$\mathbf{x}_s(s) = (s - \alpha, 0)^\top, \quad \mathbf{x}_r(s) = (s + \alpha, 0)^\top,$$

and

$$\mathbf{x}_s(\mathbf{s}) = (s_1, s_2 - \alpha, 0)^\top, \quad \mathbf{x}_r(\mathbf{s}) = (s_1, s_2 + \alpha, 0)^\top,$$

respectively.

Under these assumptions the reflection isochrones are ellipses or prolate spheroids (ellipsoids of revolution) with foci \mathbf{x}_s and \mathbf{x}_r . Further,

$$\tau(\mathbf{x}, \mathbf{y}) = |\mathbf{x} - \mathbf{y}| \quad \text{and} \quad a(\mathbf{x}, \mathbf{y}) = \begin{cases} \frac{1}{\sqrt{|\mathbf{x} - \mathbf{y}|}} & : d = 2, \\ \frac{1}{|\mathbf{x} - \mathbf{y}|} & : d = 3. \end{cases}$$

Thus, the 2D generalized Radon transform (2.9) integrates over ellipses and may be written as

$$(2.10) \quad F_2 n(s, t) = \int A_2(s, \mathbf{x}) n(\mathbf{x}) \delta(t - \varphi(s, \mathbf{x})) d\mathbf{x}, \quad t > 2\alpha,$$

with

$$\varphi(s, \mathbf{x}) := |\mathbf{x}_s(s) - \mathbf{x}| + |\mathbf{x}_r(s) - \mathbf{x}| \quad \text{and} \quad A_2(s, \mathbf{x}) = \frac{1}{\sqrt{|\mathbf{x}_s(s) - \mathbf{x}| |\mathbf{x}_r(s) - \mathbf{x}|}}.$$

The 3D generalized Radon transform (2.9) integrates over spheroids and becomes

$$(2.11) \quad F_3 n(\mathbf{s}, t) = \int A_3(\mathbf{s}, \mathbf{x}) n(\mathbf{x}) \delta(t - \varphi(\mathbf{s}, \mathbf{x})) d\mathbf{x}, \quad t > 2\alpha,$$

with

$$\varphi(\mathbf{s}, \mathbf{x}) := |\mathbf{x}_s(\mathbf{s}) - \mathbf{x}| + |\mathbf{x}_r(\mathbf{s}) - \mathbf{x}| \quad \text{and} \quad A_3(\mathbf{s}, \mathbf{x}) = \frac{1}{|\mathbf{x}_s(\mathbf{s}) - \mathbf{x}| |\mathbf{x}_r(\mathbf{s}) - \mathbf{x}|}.$$

The lower bound on t is needed because the major axis of the ellipse/spheroid must be longer than half the distance between the foci. We define the data space

$$Y = S_0 \times (2\alpha, \infty)$$

where $S_0 \subset \mathbb{R}^{d-1}$ is the bounded open set containing the parameters for the source-receiver pairs used in collecting the seismic data. Note that we are assuming the dimension $d \in \{2, 3\}$, and F_d is the forward operator in dimension d .

For later use, we give the FIO representation of F_3 :

$$(2.12) \quad F_3 n(\mathbf{s}, t) = \int \frac{1}{2\pi} A_3(\mathbf{s}, \mathbf{x}) n(\mathbf{x}) e^{i\phi(\mathbf{s}, t, \mathbf{x}, \omega)} d\mathbf{x} d\omega, \quad t > 2\alpha,$$

where $\phi(\mathbf{s}, t, \mathbf{x}, \omega) = \omega(t - \varphi(\mathbf{s}, \mathbf{x}))$.

3. THE IMAGING OPERATORS

As in [14], because there is no inversion formula in general, we do not try to reconstruct n directly from its integrals $g = F_d n$. Instead we define an imaging operator

$$(3.1) \quad K F_d^\dagger \psi F_d$$

where $\psi: Y \rightarrow [0, \infty)$ is a smooth compactly supported cutoff function and K is a properly supported pseudodifferential operator on X of non-negative order m . Further, F_d^\dagger is the *generalized backprojection* operator. For instance, for $u \in \mathcal{D}(Y)$,

$$(3.2) \quad \begin{aligned} F_3^\dagger u(\mathbf{x}) &= \int_{S_0} \int_{2\alpha}^\infty W(\mathbf{s}, \mathbf{x}) u(\mathbf{s}, t) \delta(t - \varphi(\mathbf{s}, \mathbf{x})) dt d\mathbf{s} \\ &= \int_{S_0} W(\mathbf{s}, \mathbf{x}) u(\mathbf{s}, \varphi(\mathbf{s}, \mathbf{x})) d\mathbf{s} \end{aligned}$$

where W is a smooth positive weight. The 2D version F_2^\dagger of the generalized backprojection is given analogously. Then, the composition $F_d^\dagger \psi F_d$ is defined for distributions of compact support.⁴

Note that the formal L^2 -adjoint F_d^* has weight $W = A_d$ and the generalized backprojection used by Beylkin [1] has weight $W = 1/A_d$.

3.1. Pseudodifferential Operators. Our theoretical results are based on these operators, and we now introduce the building blocks.

Definition 3.1 (Pseudodifferential Symbol). Let X be an open subset of \mathbb{R}^d . A *symbol of order m* is a function $p = p(\mathbf{x}, \xi) \in C^\infty(X \times \mathbb{R}^d)$ satisfying: For every compact set $K \subset X$ and for each set of two multi-indices α, β there exists a constant $C = C(K, \alpha, \beta)$ such that, for all $\mathbf{x} \in K$ and all $\xi \in \mathbb{R}^d$,

$$|D_\xi^\alpha D_{\mathbf{x}}^\beta p(\mathbf{x}, \xi)| \leq C(1 + |\xi|)^{m - |\alpha|}.$$

The set of symbols of order m above X is denoted $S^m(X)$.

The symbol p is *elliptic* if for each compact subset K of X there are positive constants c and M such that

$$(3.3) \quad |p(\mathbf{x}, \xi)| \geq c(1 + |\xi|)^m$$

for all $\mathbf{x} \in K$ and all ξ with $|\xi| \geq M$.

Let $(\mathbf{x}_0, \xi_0) \in X \times (\mathbb{R}^d \setminus \{\mathbf{0}\})$. Then, the symbol p is *microlocally elliptic near (\mathbf{x}_0, ξ_0)* if there are an open neighborhood U of \mathbf{x}_0 , a conic open neighborhood V of ξ_0 , and positive constants C and M such that (3.3) holds for all $\mathbf{x} \in U$ and $\xi \in V$ with $|\xi| \geq M$.

Definition 3.2 (Pseudodifferential operator). Let X be an open subset of \mathbb{R}^d and $m \in \mathbb{R}$. Then, the linear operator $P: \mathcal{D}(X) \rightarrow \mathcal{E}(X)$ is a *pseudodifferential operator of order m* if there is a pseudodifferential symbol p of order m such that for all $f \in \mathcal{D}(X)$,

$$Pf(\mathbf{y}) = \int_{\mathbb{R}^d} \int_X e^{i(\mathbf{y} - \mathbf{x}) \cdot \xi} p(\mathbf{x}, \xi) f(\mathbf{x}) d\mathbf{x} d\xi.$$

The function p is called the *full symbol* of the operator P . The *top order symbol* $\sigma(P)$ of P is the equivalence class of p in the quotient space $S^m(X)/S^{m-1}(X)$.

The operator P is *elliptic* (respectively: *microlocally elliptic*) if its symbol is elliptic (respectively: microlocally elliptic).

⁴We emphasize that $F_d^* F_d$ is not defined in general because $F_d: \mathcal{D}'(X) \rightarrow \mathcal{D}'(Y)$ but $F_d^*: \mathcal{E}'(Y) \rightarrow \mathcal{D}'(X)$. Therefore, throughout this article, we let ψ be a smooth cutoff function of compact support in Y and we consider only operators that include ψ , such as $F_d^* \psi F_d$ and $F_d^\dagger \psi F_d$.

Let P be a Ψ DO of order m . When we write $\sigma(P)$ as a function, we understand this as the equivalence class of the function modulo $S^{m-1}(X)$. We will introduce some more technical terminology in Section 5.

3.2. Main Theorems. Our first theorem explains our choice (3.1) of the imaging operator. It follows from arguments in [21] and [8].

Theorem 3.3. *Let F_d , F_d^\dagger , K , and ψ be defined as above. Then,*

$$KF_d^\dagger \psi F_d \text{ and } KF_d^* \psi F_d$$

are Ψ DOs of order $m + 1 - d$.

Proof. We consider $KF_d^\dagger \psi F_d$ and note that the other operator is just a special case.

First, let $d = 3$. In [8], it was shown that F_3 is an FIO. Let \mathcal{C} be the canonical relation of F_3 . Then, F_3^* is an FIO with canonical relation \mathcal{C}^t [20], and F_3^\dagger is essentially the same operator, but with a different weight, so it has the same canonical relation. The operator F_3 has symbol $A_3/(2\pi)$ which is homogeneous of order zero in the phase variable, ω , by (2.12). The dimension of the ambient spaces is three and the dimension of phase space is 1. Therefore, the order of F_3 is $-(3 - 1)/2 = -1$ [38, p. 462 below (6.3)]. Since the symbol of F_3^\dagger is homogeneous of order zero in the phase variable, the same calculation as for F_3 shows F_3^\dagger is an FIO of order -1 with canonical relation \mathcal{C}^t . Multiplication by ψ does not affect the order of an FIO, so $F_3^\dagger \psi F_3$ has canonical relation $\mathcal{C}^t \circ \mathcal{C}$ and order -2 . However, the microlocal Bolker assumption (see (5.18) and e.g., [17, p. 371]) is satisfied by F_3 and \mathcal{C} [8], so $\mathcal{C}^t \circ \mathcal{C}$ is a subset of the diagonal. Therefore, $F_d^\dagger \psi F_3$ is a Ψ DO. Because K is a Ψ DO of order m , and the composition of Ψ DOs is a Ψ DO, $KF_3^\dagger \psi F_3$ is a Ψ DO of order $m - 2$.

Similar reasoning holds in case $d = 2$. In this case, the needed Bolker assumption follows from [21, Theorem 4]. Since the symbol of F_2 is homogenous of degree zero, F_2 has order $-(2 - 1)/2 = -1/2$. Since F_2 satisfies the microlocal Bolker assumption, $F_2^\dagger \psi F_2$ is a Ψ DO of order -1 . Since K is a Ψ DO of order m , $KF_2^\dagger \psi F_2$ has order $m - 1$. \square

The above theorem states that the operators

$$KF_d^\dagger \psi g \text{ and } KF_d^* \psi g$$

are Ψ DOs, and therefore some singularities of n can be visible in the reconstructions, and artifacts are not added to the reconstruction because of the smooth cutoff ψ (see e.g., [10] for an analysis when cutoffs are not smooth). If $m > d - 1$ the reconstruction operators have positive order and, thus, the singularities are even emphasized.

Beylkin [1] established F_3^\dagger with weight $W = 1/A_3$ as imaging operator and showed that there is a convolution operator P such that

$$F_3^\dagger P F_3 = I_{\text{partial}} + \Psi$$

where the partial identity I_{partial} is a kind of band pass filter and Ψ is of lower order.

Our imaging operators are more general and we compute their symbols below in order to understand how they map singularities, in particular, how they might emphasize or de-emphasize singularities.

The next lemma gives important technical information for the three-dimensional case.

Lemma 3.4. *Let $\mathbf{x} \in X$ and $\xi \in \mathbb{R}^3 \setminus \{\mathbf{0}\}$ with $\xi_3 \neq 0$. Then, the equation*

$$(3.4) \quad (\xi_1, \xi_2, \xi_3) = \omega \nabla_{\mathbf{x}} \varphi(\mathbf{s}, \mathbf{x})$$

uniquely determines $\omega \neq 0$ and $\mathbf{s} = (s_1, s_2) \in \mathbb{R}^2$ as functions of (\mathbf{x}, ξ) . They are given by (5.4), (5.5), and (5.9) respectively.

We write $\mathbf{s} = \mathbf{s}(\mathbf{x}, \xi)$ and $\omega = \omega(\mathbf{x}, \xi)$ for $\mathbf{x} \in X$ and $\xi \in \mathbb{R}^3 \setminus \{\mathbf{0}\}$ with $\xi_3 \neq 0$.

This lemma is proved in Section 5.1.

Our next theorems provide the symbols of our imaging operators and will allow us to analyze which singularities are visible in the reconstruction and to choose an effective operator K . The proofs, which use the theory of Fourier integral operators, are in Section 5.

Theorem 3.5 (3D-Symbol for Common Offset). *Let K be a properly supported ΨDO with symbol $k(\mathbf{x}, \xi)$ and let F_3^\dagger have smooth weight W . The top order symbol of $K F_3^\dagger \psi F_3$ as a pseudodifferential operator is*

$$(3.5) \quad \sigma(K F_3^\dagger \psi F_3)(\mathbf{x}, \xi) = \frac{(2\pi)^2 k(\mathbf{x}, \xi) \psi(\mathbf{s}, \varphi(\mathbf{s}, \mathbf{x})) W(\mathbf{s}, \mathbf{x}) A_3(\mathbf{s}, \mathbf{x})}{|\omega|^2 B_3(\mathbf{s}, \mathbf{x})}$$

where B_3 is the Beylkin determinant [1] given by

$$(3.6) \quad B_3(\mathbf{s}, \mathbf{x}) = \left| \det \begin{pmatrix} \nabla_{\mathbf{x}} \varphi(\mathbf{s}, \mathbf{x}) \\ \frac{\partial}{\partial s_1} \nabla_{\mathbf{x}} \varphi(\mathbf{s}, \mathbf{x}) \\ \frac{\partial}{\partial s_2} \nabla_{\mathbf{x}} \varphi(\mathbf{s}, \mathbf{x}) \end{pmatrix} \right|.$$

This symbol is evaluated at (\mathbf{x}, ξ) and $\mathbf{s} = \mathbf{s}(\mathbf{x}, \xi)$ and $\omega = \omega(\mathbf{x}, \xi)$ satisfy (3.4) in Lemma 3.4.

The top order symbol of $K F_3^* \psi F_3$ as a pseudodifferential operator is

$$(3.7) \quad \sigma(K F_3^* \psi F_3)(\mathbf{x}, \xi) = \frac{(2\pi)^2 k(\mathbf{x}, \xi) \psi(\mathbf{s}, \varphi(\mathbf{s}, \mathbf{x})) A_3^2(\mathbf{s}, \mathbf{x})}{|\omega|^2 B_3(\mathbf{s}, \mathbf{x})}$$

where $\mathbf{s} = \mathbf{s}(\mathbf{x}, \xi)$ and $\omega = \omega(\mathbf{x}, \xi)$.

This theorem is proved in Section 5.2. The proof is valid for any Radon transform defined by a function φ (or any FIO associated to the canonical relation \mathcal{C} of such an operator), as long as \mathcal{C} satisfies the Bolker assumption (see (5.18) and [17, p. 371]), and a proof will be given elsewhere. Observe that B_3 does not vanish whenever the Bolker assumption holds.

Our next lemma is the two-dimensional version of Lemma 3.4.

Lemma 3.6. *Let $\mathbf{x} \in X$ and $\xi \in \mathbb{R}^2 \setminus \{\mathbf{0}\}$ with $\xi_2 \neq 0$. Then, the equation*

$$(3.8) \quad (\xi_1, \xi_2) = \omega \nabla_{\mathbf{x}} \varphi(\mathbf{s}, \mathbf{x})$$

uniquely determines $s \in \mathbb{R}$ and $\omega \neq 0$ as functions of (\mathbf{x}, ξ) . They are given by (5.11) and (5.10) respectively.

We write $s = s(\mathbf{x}, \xi)$ and $\omega = \omega(\mathbf{x}, \xi)$ for $\mathbf{x} \in X$ and $\xi \in \mathbb{R}^2 \setminus \{\mathbf{0}\}$ with $\xi_2 \neq 0$.

The proof of this lemma is analogous to the proof of Lemma 3.4. See Figure 1 for a geometric picture of the solution of equation (3.8).

Theorem 3.7 (2D-Symbol for Common Offset). *Under the assumptions of the previous theorem the 2D-symbols are*

$$(3.9) \quad \sigma(K F_2^\dagger \psi F_2)(\mathbf{x}, \xi) = \frac{2\pi k(\mathbf{x}, \xi) \psi(s, \varphi(s, \mathbf{x})) W(s, \mathbf{x}) A_2(s, \mathbf{x})}{|\omega| B_2(s, \mathbf{x})}$$

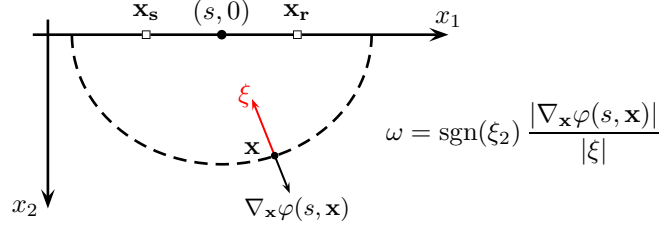


FIGURE 1. Illustration of (3.8). The geometric steps to solve this equation are as follows: First determine an ellipse which passes through \mathbf{x} and is normal to ξ at \mathbf{x} . So we found s . Then, ω is just the scale factor in $\xi = \omega \nabla_{\mathbf{x}} \varphi(s, \mathbf{x})$.

and

$$(3.10) \quad \sigma(KF_2^* \psi F_2)(\mathbf{x}, \xi) = \frac{2\pi k(\mathbf{x}, \xi) \psi(s, \varphi(s, \mathbf{x})) A_2^2(s, \mathbf{x})}{|\omega| B_2(s, \mathbf{x})}$$

where

$$(3.11) \quad B_2(s, \mathbf{x}) = \left| \det \begin{pmatrix} \nabla_{\mathbf{x}} \varphi(s, \mathbf{x}) \\ \frac{\partial}{\partial s} \nabla_{\mathbf{x}} \varphi(s, \mathbf{x}) \end{pmatrix} \right|$$

with $s \in \mathbb{R}$ and $\omega \neq 0$ uniquely defined by $(\xi_1, \xi_2) = \omega \nabla_{\mathbf{x}} \varphi(s, \mathbf{x})$.

In Section 4.1, we will derive a simpler expression for (3.10).

4. IMAGING IN 2D

Here we demonstrate how we benefit from the symbol calculation for a concrete imaging situation. For the ease of presentation we restrict ourselves to the two-dimensional setting. The calculations as well as consequences for the three-dimensional situation will be published elsewhere.

4.1. The symbol in 2D. We first consider the operator $\Lambda = \Delta_{\mathbf{x}} F_2^* \psi F_2$, where $\Delta_{\mathbf{x}}$ is the Laplacian and express its top order symbol $\sigma(\Lambda)$ in terms of $\mathbf{x} \in X$ and $\xi \in \mathbb{R}^2 \setminus \{\mathbf{0}\}$ with $\xi_2 \neq 0$. The final expression for the symbol is given in Proposition 4.1. Then, we use this to analyze ellipticity of this operator and come up with an improved operator in Section 4.2.

We recall the symbol for a general operator $KF_2^* \psi F_2$. According to (3.10) (with $k = 1$) we have that

$$\sigma(F_2^* \psi F_2)(\mathbf{x}, \xi) = -2\pi |\xi|^2 \frac{\psi(s, \varphi(s, \mathbf{x})) A_2^2(s, \mathbf{x})}{|\omega| B_2(s, \mathbf{x})}.$$

With the notation

$$(4.1) \quad \ell := x_1 - s, \quad D := \sqrt{(\ell - \alpha)^2 + x_2^2}, \quad \text{and} \quad E := \sqrt{(\ell + \alpha)^2 + x_2^2}$$

we get

$$\nabla_{\mathbf{x}} \varphi(s, \mathbf{x}) = \begin{pmatrix} \frac{\ell - \alpha}{D} + \frac{\ell + \alpha}{E} \\ x_2 \left(\frac{1}{D} + \frac{1}{E} \right) \end{pmatrix} \quad \text{and} \quad \partial_s \nabla_{\mathbf{x}} \varphi(s, \mathbf{x}) = \begin{pmatrix} -\frac{x_2^2}{D^3} - \frac{x_2^2}{E^3} \\ x_2 \left(\frac{\ell - \alpha}{D^3} + \frac{\ell + \alpha}{E^3} \right) \end{pmatrix}.$$

Now,

$$\begin{aligned} |\omega|B_2(s, \mathbf{x}) &= \left| \det \left(\omega \nabla_{\mathbf{x}} \varphi(s, \mathbf{x}), \partial_s \nabla_{\mathbf{x}} \varphi(s, \mathbf{x}) \right) \right| \stackrel{(3.8)}{=} \left| \det \left(\xi, \partial_s \nabla_{\mathbf{x}} \varphi(s, \mathbf{x}) \right) \right| \\ &= x_2 |\xi_2| \left| q \left(\frac{\ell - \alpha}{D^3} + \frac{\ell + \alpha}{E^3} \right) + x_2 \left(\frac{1}{D^3} + \frac{1}{E^3} \right) \right| \end{aligned}$$

where

$$(4.2) \quad q := \xi_1 / \xi_2.$$

Further,

$$\begin{aligned} \frac{A_2^2(s, \mathbf{x})}{|\omega|B_2(s, \mathbf{x})} &= \frac{1}{ED} \frac{1}{x_2 |\xi_2| \left| q \left(\frac{\ell - \alpha}{D^3} + \frac{\ell + \alpha}{E^3} \right) + x_2 \left(\frac{1}{D^3} + \frac{1}{E^3} \right) \right|} \\ &= \frac{1}{x_2 |\xi_2| \left| q \left((\ell - \alpha) \frac{E}{D^2} + (\ell + \alpha) \frac{D}{E^2} \right) + x_2 \left(\frac{E}{D^2} + \frac{D}{E^2} \right) \right|}. \end{aligned}$$

In view of (5.11) and using the abbreviation

$$Q(q, \lambda) := \frac{1}{2q} \left(q^2 - 1 + \sqrt{(q^2 + 1)^2 + 4\lambda^2 q^2} \right)$$

we may write ℓ , D , and E as functions of \mathbf{x} and ξ :

$$\begin{aligned} \ell &= x_2 Q(q, \frac{\alpha}{x_2}), \quad D = x_2 \sqrt{\left(Q(q, \frac{\alpha}{x_2}) - \frac{\alpha}{x_2} \right)^2 + 1}, \\ E &= x_2 \sqrt{\left(Q(q, \frac{\alpha}{x_2}) + \frac{\alpha}{x_2} \right)^2 + 1}. \end{aligned}$$

Proposition 4.1. *The top order symbol of $\Lambda = \Delta_{\mathbf{x}} F_2^* \psi F_2$ is*

$$(4.3) \quad \sigma(\mathbf{x}, \xi) := \sigma(\Lambda)(\mathbf{x}, \xi) = - \frac{2\pi |\xi|^2 \psi(x_1 - x_2 Q(q, \frac{\alpha}{x_2}), D + E)}{x_2 |\xi_2| \left| q \left((\ell - \alpha) \frac{E}{D^2} + (\ell + \alpha) \frac{D}{E^2} \right) + x_2 \left(\frac{E}{D^2} + \frac{D}{E^2} \right) \right|}$$

where ℓ , D , and E are given by (4.1) and q is given by (4.2).

Note that the right hand side of (4.3) is expressed exclusively in terms of \mathbf{x} and ξ (recall that $q = \xi_1 / \xi_2$). We see that $\sigma = \sigma(\Lambda)$ is positively homogeneous of order 1 in ξ which reflects the order of Λ . Further, the arguments in our proof also show that the symbol of $K F_2^* \psi F_2$ is (4.3) with $|\xi|^2$ replaced by k , the symbol of K .

Based on (4.3) we describe in Corollary 4.3 below precisely where and how Λ emphasizes singularities. To this end we need to introduce some additional terminology, see e.g. [25] for more details.

Definition 4.2 (H^r -Wavefront Set). i) Let $r \in \mathbb{R}$. We say that $u \in \mathcal{D}'(X)$ is (microlocally) H^r at $(\mathbf{x}_o, \eta_o) \in X \times (\mathbb{R}^d \setminus \{\mathbf{0}\})$ if the following holds: for some neighborhood U of \mathbf{x}_o and some conic neighborhood V of η_o we have that

$$\int_V |\widehat{\varphi u}(\xi)|^2 (1 + |\xi|^2)^r d\xi < \infty$$

for one $\varphi \in \mathcal{D}(U)$ with $\varphi(\mathbf{x}_o) \neq 0$. Here, \widehat{w} denotes the Fourier transform of the tempered distribution w .

ii) The H^r -wave front set $\text{WF}^r(u)$ of $u \in \mathcal{D}'(X)$ is the complement in $X \times (\mathbb{R}^d \setminus \{\mathbf{0}\})$ of the set of all points $(\mathbf{x}_o, \eta_o) \in X \times (\mathbb{R}^d \setminus \{\mathbf{0}\})$ where u is H^r .

Now we use (4.3) to determine where our operator is microlocally elliptic, see Definitions 3.1 and 3.2. This provides a quantitative relation, (4.4), between the strength of the singularities for u and those of Λu .

Corollary 4.3. *For $\mathbf{x} \in X$ let*

$$C(\mathbf{x}) = \left\{ \xi \in \mathbb{R}^2 : \xi_2 \neq 0, \psi\left(x_1 - x_2 Q\left(q, \frac{\alpha}{x_2}\right), D + E\right) > 0 \right\}.$$

Consider $(\mathbf{y}, \eta) \in X \times (\mathbb{R}^2 \setminus \{\mathbf{0}\})$ with $\eta \in C(\mathbf{y})$. Then, Λ is microlocally elliptic of order 1 at (\mathbf{y}, η) . Further, for any $u \in \mathcal{E}(X)$,

$$(4.4) \quad (\mathbf{y}, \eta) \in \text{WF}^r(u) \iff (\mathbf{y}, \eta) \in \text{WF}^{r-1}(\Lambda u).$$

Proof. First, let $\eta_1 > 0$. Define $\overline{m} := \eta_2/\eta_1$ and the cone

$$V_\epsilon = \left\{ (\lambda, m\lambda)^\top : \lambda \geq 0, m \in [\overline{m} - \epsilon, \overline{m} + \epsilon] \right\}$$

where ϵ is chosen small enough so that $0 < \epsilon < |\overline{m}|$. Obviously, V_ϵ is a conic neighborhood of η . Further, for $0 \neq \xi \in V_\epsilon$ we have that

$$\frac{1}{\overline{m} + \epsilon} \leq q = \frac{\xi_1}{\xi_2} \leq \frac{1}{\overline{m} - \epsilon}.$$

Let B_ϱ be the closed ball about \mathbf{y} in \mathbb{R}_+^2 with radius $\varrho > 0$. By continuity we may decrease ϵ and ϱ so that

$$\min \left\{ \frac{2\pi \psi\left(x_1 - x_2 Q\left(q, \frac{\alpha}{x_2}\right), D + E\right)}{x_2 \left| q \left((\ell - \alpha) \frac{E}{D^2} + (\ell + \alpha) \frac{D}{E^2} \right) + x_2 \left(\frac{E}{D^2} + \frac{D}{E^2} \right) \right|} : \right. \\ \left. 0 \neq \xi \in V_\epsilon, \mathbf{x} \in B_\varrho \right\} =: c_{\epsilon, \varrho} > 0.$$

Hence,

$$|\sigma(\mathbf{x}, \xi)| \geq c_{\epsilon, \varrho} \frac{|\xi|}{|\xi_2|} |\xi| \geq c_{\epsilon, \varrho} |\xi| \quad \text{for all } \mathbf{x} \in B_\varrho \text{ and } \xi \in V_\epsilon$$

where σ is the symbol of Λ . If $\eta_1 = 0$, $\eta_2 \geq 0$, we define $V_\epsilon = \{(m\lambda, \lambda)^\top : \lambda \geq 0, m \in [-\epsilon, \epsilon]\}$ and proceed as above. For $\eta_1 = 0$, $\eta_2 < 0$ the conic neighborhood $V_\epsilon = \{(m\lambda, -\lambda)^\top : \lambda \geq 0, m \in [-\epsilon, \epsilon]\}$ will do the job. Similar arguments work in case $\eta_1 < 0$.

The proof of the second statement of the corollary uses arguments in [25, p. 259 ff.], and it is done in the same way as the proof of the last assertion of Theorem 3.1 in [27]. \square

4.2. An improved reconstruction operator in 2D. The symbol of the operator Λ has a factor of $1/x_2$ which de-emphasizes features far from the surface—when x_2 is large. We will now analyze the symbol of operator $\Lambda = \Delta_{\mathbf{x}} F^* \psi F$ asymptotically as $\alpha \rightarrow 0$ (or equivalently, as $x_2 \rightarrow \infty$), in order to form an operator that reconstructs features more uniformly, independent of the depth (value of x_2) and distance between the source and receiver, 2α .

We want to find more explicit expressions for σ in certain ranges of α . For $\alpha = 0$ we get

$$\sigma(\mathbf{x}, \xi) = -\pi \frac{|\xi|}{x_2} \psi\left(x_1 - \frac{\xi_1}{\xi_2} x_2, 2x_2 \frac{|\xi|}{|\xi_2|}\right).$$

It is clear from the above representations of ℓ , D , and E that

$$(4.5) \quad \sigma(\mathbf{x}, \xi) \approx -\pi \frac{|\xi|}{x_2} \psi\left(x_1 - \frac{\xi_1}{\xi_2} x_2, 2x_2 \frac{|\xi|}{|\xi_2|}\right) \quad \text{for } x_2 \gg \alpha$$

(ellipses with major diameter much larger than α look like circles). Since

$$(4.6) \quad \sigma(\mathbf{x}, (0, \xi_2)) = -\pi |\xi_2| \frac{\sqrt{\alpha^2 + x_2^2}}{x_2^2} \psi\left(x_1, 2\sqrt{\alpha^2 + x_2^2}\right)$$

we assume $\xi_1 \neq 0$ in the sequel, that is, $q \neq 0$.

Now, we want to get an asymptotic expression for the symbol in case $\alpha \gg x_2$. This corresponds to features near the surface. Let $q > 0$. As

$$\lim_{\alpha \rightarrow \infty} \left(Q(q, \frac{\alpha}{x_2}) - \frac{\alpha}{x_2}\right) = (q^2 - 1)/(2q) =: C_q$$

we get

$$\lim_{\alpha \rightarrow \infty} D = x_2 \sqrt{C_q^2 + 1}.$$

Further, since

$$Q(q, \lambda) \asymp \lambda \text{ as } \lambda \rightarrow \infty \text{ (asymptotically equal)}$$

we find

$$E \asymp 2\alpha \quad \text{for large } \alpha \quad \text{and} \quad \lim_{\alpha \rightarrow \infty} (\ell - \alpha) = C_q x_2.$$

Hence,

$$(\ell - \alpha) \frac{E}{D^2} \asymp \frac{2C_q}{C_q^2 + 1} \frac{\alpha}{x_2}$$

and

$$\lim_{\alpha \rightarrow \infty} (\ell + \alpha) \frac{D}{E^2} = 0.$$

Also,

$$\frac{E}{D^2} \asymp \frac{2}{C_q^2 + 1} \frac{\alpha}{x_2^2} \quad \text{and} \quad \frac{D}{E^2} \asymp \sqrt{C_q^2 + 1} \frac{x_2}{4\alpha^2}.$$

Thus,

$$\begin{aligned} x_2 |\xi_2| \left| q \left((\ell - \alpha) \frac{E}{D^2} + (\ell + \alpha) \frac{D}{E^2} \right) + x_2 \left(\frac{E}{D^2} + \frac{D}{E^2} \right) \right| \\ \asymp x_2 |\xi_2| \left| q \frac{2C_q}{C_q^2 + 1} \frac{\alpha}{x_2} + \frac{2}{C_q^2 + 1} \frac{\alpha}{x_2} \right| = 4\alpha \frac{|\xi_2| |\xi_1|^2}{|\xi|^2}. \end{aligned}$$

The above asymptotic result is true also in case $q < 0$ (the roles of D and E as well as of $\ell - \alpha$ and $\ell + \alpha$ just interchange).

Combining all ingredients we get

$$(4.7) \quad \sigma(\mathbf{x}, \xi) \approx -\frac{\pi}{2} \frac{|\xi|^4}{|\xi_2| |\xi_1|^2} \frac{1}{\alpha} \psi\left(x_1 - \alpha, 2\alpha + x_2 \frac{|\xi|^2}{2|\xi_1 \xi_2|}\right) \quad \text{for } \alpha \gg x_2.$$

In view of our explicit expressions for the symbol of Λ we propose the modified imaging operator

$$\Lambda_{\text{mod}, \beta} = \Delta(M + \beta \text{Id}) F_2^* \psi F_2$$

where M is the multiplication operator with x_2 and $\beta \geq 0$. The top order symbol of $\Lambda_{\text{mod}, \beta}$ is $(x_2 + \beta)\sigma(\mathbf{x}, \xi)$. What would be a good choice for β ? Please note that in case of $\alpha = 0$ the symbol of $\Lambda_{\text{mod}, \alpha}$ does not contain the factor $1/x_2$ anymore. As a consequence, jumps in n with the same height but at different depths will be reconstructed with the same intensities. By the choice $\beta = \alpha$ the same property holds

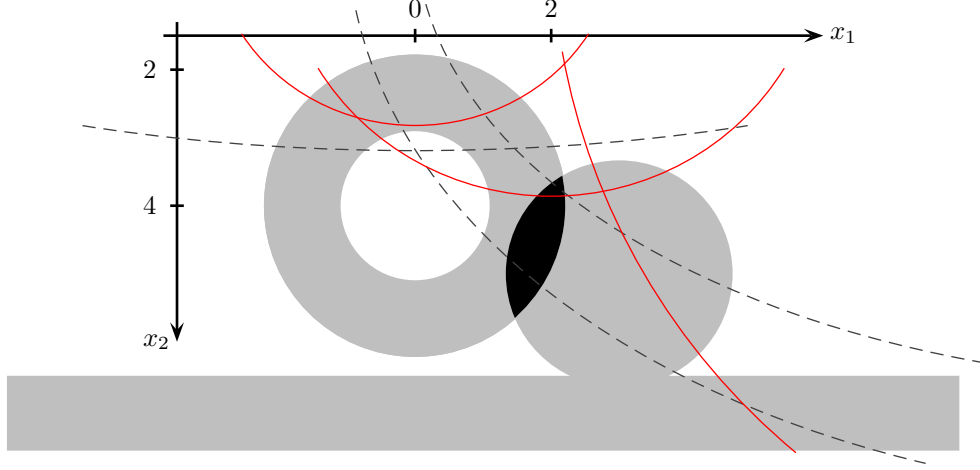


FIGURE 2. Visualization of the function n (4.8). Light gray area: $n = 1$, black: $n = 2$, white: $n = 0$. The light gray bar represents the half space $x_2 \geq 6.5$. The three dashed curves show elliptic arcs belonging to the common offset $\alpha = 10$ and $s = 0, t = 21$; $s = 12, t = 24$; $s = 12, t = 26$. The three solid red lines show elliptic arcs for $\alpha = 1$ where $s = 0, t = 6$; $s = 2, t = 8$; $s = 12, t = 20$.

approximately for $\alpha > 0$ because the factor $x_2 + \alpha$ compensates for $1/x_2$ if $x_2 \gg \alpha$ and for $1/\alpha$ if $x_2 \ll \alpha$, see (4.5) and (4.7).

4.3. Numerical illustrations. We present numerical experiments to compare different imaging operators under different scenarios. We use the reconstruction algorithm developed in [14] to compute approximations to Λn and $\Lambda_{\text{mod},\beta} n$ from the elliptic means $F_2 n(s_i, t_j)$, $i = 1, \dots, N_s$, $j = 1, \dots, N_t$, where $\{s_i\} \subset [-s_{\max}, s_{\max}]$ and $\{t_j\} \subset [t_{\min}, t_{\max}]$, $t_{\min} > 2\alpha$, are equidistantly distributed.

The function n is given by a superposition of indicator functions of balls and a half-space:

$$(4.8) \quad n = \chi_{B((0,4),2)} - \chi_{B((0,4),1)} + \chi_{B((3,5),1.5)} + \chi_{x_2 \geq 6.5},$$

see Figure 2. The numerical values $\psi(s_i, t_j) F_2 n(s_i, t_j)$ have been calculated semi-analytically as explained in [14, Section 3] using the cutoff function defined on the bottom of p. 12 of [14].

In Figure 3 the offset is $\alpha = 1$. Further, $s_{\max} = 12$, $N_s = 300$, $N_t = 200$, $t_{\min} = 4$, and $t_{\max} = 19$. As the singular support of n is contained in the strip $\mathbb{R} \times [2, 6.5]$ we are in the regime $x_2 \gg \alpha$, that is, the symbol of Λ is given by (4.5). Ellipses intersecting the support of n look like circles, see the solid red curves in Figure 2. In the top image of Figure 3, which shows Λn , we clearly see that the intensities of the reconstructed jumps decrease with increasing x_2 . The middle image presents $\Lambda_{\text{mod},0} n$. Here, the dependence on x_2 is not as strong as for Λn but now singularities closer to the surface are reconstructed with slightly weaker intensities. A depth-independent reconstruction yields $\Lambda_{\text{mod},\alpha}$, see bottom image.

In the next set of experiments we have chosen $\alpha = 10$. Further, $s_{\max} = 15$, $N_s = N_t = 600$, $t_{\min} = 20.2$, and $t_{\max} = 35.2$. As $\alpha \gg x_2$ and $x_2 \in \text{sing supp } n$ we are in

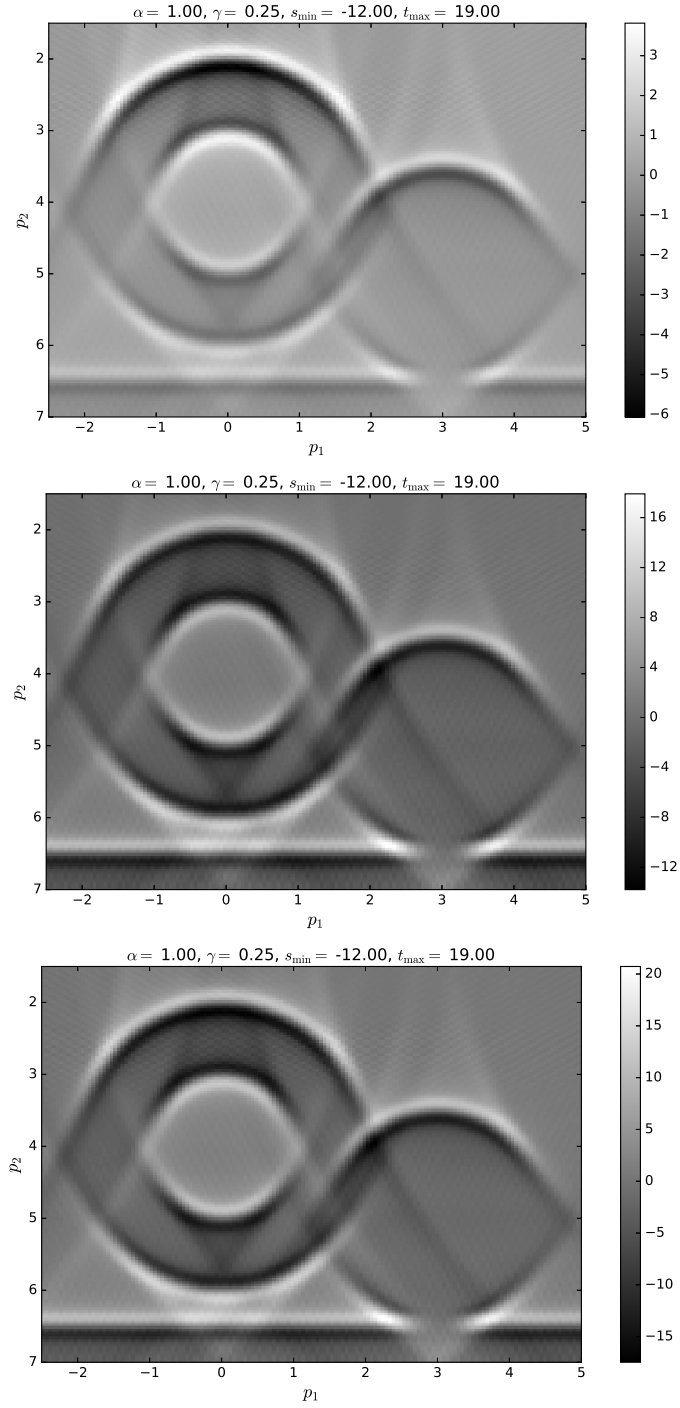


FIGURE 3. Reconstructions for offset $\alpha = 1$. Top: Λn , middle: $\Lambda_{\text{mod},0} n$, bottom: $\Lambda_{\text{mod},\alpha} n$

scenario (4.7), that is, Λn exhibits a moderate depth-dependence in the reconstruction of the singular support of n (top of Figure 4). Now, $\Lambda_{\text{mod},0}n$ (middle of Figure 4) shows depth-dependence: jumps farther down are emphasized more with increasing x_2 . By and large, only $\Lambda_{\text{mod},\alpha}$ exhibits depth-independence (bottom of Figure 4).

5. PROOFS

5.1. The Basic Geometry, Proofs of Lemmas 3.4 and 3.6. First we prove Lemma 3.4. We explicitly solve (3.4) for $\mathbf{s} = (s_1, s_2)$ and ω . Let $\mathbf{x} \in X$ and $\xi \in \mathbb{R}^3 \setminus \{\mathbf{0}\}$ with $\xi_3 \neq 0$. Then, we have to solve the nonlinear system of equations

$$(5.1) \quad \omega(x_1 - s_1) \left(\frac{1}{D} + \frac{1}{E} \right) = \xi_1,$$

$$(5.2) \quad \omega \left(\frac{x_2 - s_2 - \alpha}{D} + \frac{x_2 - s_2 + \alpha}{E} \right) = \xi_2,$$

$$(5.3) \quad \omega x_3 \left(\frac{1}{D} + \frac{1}{E} \right) = \xi_3,$$

where

$$D = \sqrt{(\ell - \alpha)^2 + \beta^2} \quad \text{and} \quad E = \sqrt{(\ell + \alpha)^2 + \beta^2},$$

with $\ell := x_2 - s_2$ and $\beta^2 := (x_1 - s_1)^2 + x_3^2 > 0$.

Equation (5.3) yields that

$$(5.4) \quad \omega = \frac{\xi_3}{x_3 \left(\frac{1}{D} + \frac{1}{E} \right)}.$$

We plug this expression for ω into the first two equations. From (5.1) we then immediately obtain that

$$(5.5) \quad s_1 = x_1 - \frac{\xi_1 x_3}{\xi_3}.$$

With s_1 given, so is β^2 . Equation (5.2) – using (5.4) – now reads

$$(5.6) \quad g(\ell) = \frac{\xi_2 x_3}{\xi_3},$$

where the function $g: \mathbb{R} \rightarrow \mathbb{R}$,

$$(5.7) \quad g(\ell) := \frac{\sqrt{(\ell + \alpha)^2 + \beta^2}(\ell - \alpha) + \sqrt{(\ell - \alpha)^2 + \beta^2}(\ell + \alpha)}{\sqrt{(\ell - \alpha)^2 + \beta^2} + \sqrt{(\ell + \alpha)^2 + \beta^2}},$$

is invertible. Indeed,

$$(5.8) \quad g^{-1}(\delta) = \begin{cases} \frac{\delta^2 - \beta^2 + \sqrt{(\delta^2 + \beta^2)^2 + 4\alpha^2\delta^2}}{2\delta} & : \delta \neq 0, \\ 0 & : \delta = 0. \end{cases}$$

The proof is below. Thus, $s_2 = x_2 - \ell$ is explicitly given by

$$(5.9) \quad s_2 = \begin{cases} x_2 - \frac{1}{2} \frac{\xi_3}{\xi_2} \left(x_3 \left(\frac{\xi_2^2 - \xi_1^2}{\xi_3^2} - 1 \right) + \sqrt{x_3^2 \left(1 + \frac{\xi_1^2 + \xi_2^2}{\xi_3^2} \right)^2 + 4\alpha^2 \frac{\xi_2^2}{\xi_3^2}} \right) & : \xi_2 \neq 0, \\ x_2 & : \xi_2 = 0. \end{cases}$$

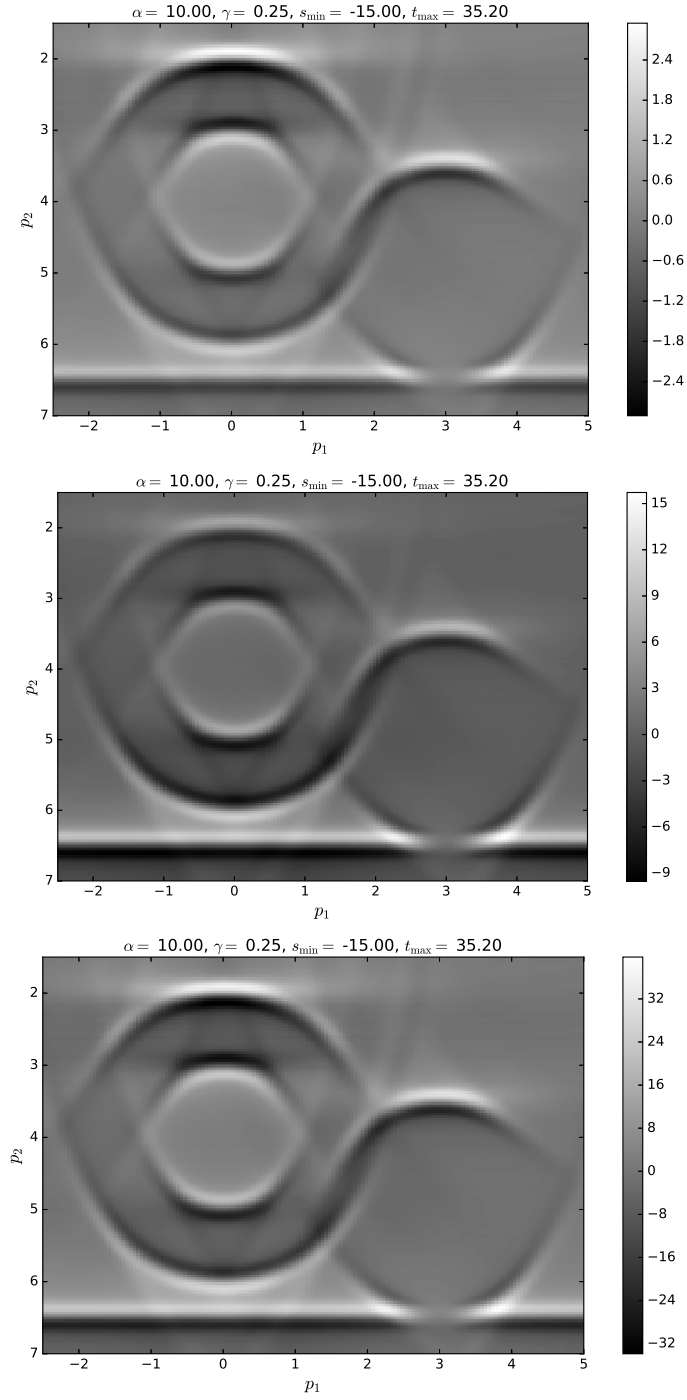


FIGURE 4. Reconstructions for offset $\alpha = 10$. Top: Λn , middle: $\Lambda_{\text{mod},0} n$, bottom: $\Lambda_{\text{mod},\alpha} n$

The representation of ω in (5.4) still depends on (s_1, s_2) via D , E and ℓ . With the above values for (s_1, s_2) we can express ω exclusively by \mathbf{x} and ξ .

It remains to prove (5.8). First, we show that g is injective. We have that

$$g'(\ell) = \frac{2(\alpha^2 + \beta^2 + \ell^2)(\ell^2 - \alpha^2 + \sqrt{(\ell - \alpha)^2 + \beta^2} \sqrt{(\ell + \alpha)^2 + \beta^2} + \beta^2)}{\sqrt{(\ell - \alpha)^2 + \beta^2} \sqrt{(\ell + \alpha)^2 + \beta^2} (\sqrt{(\ell - \alpha)^2 + \beta^2} + \sqrt{(\ell + \alpha)^2 + \beta^2})^2}.$$

It holds that

$$g'(\ell) > 0 \iff \ell^2 - \alpha^2 + \sqrt{(\ell - \alpha)^2 + \beta^2} \sqrt{(\ell + \alpha)^2 + \beta^2} + \beta^2 > 0.$$

Let us consider the expression

$$\ell^2 - \alpha^2 + \sqrt{(\ell - \alpha)^2 + \beta^2} \sqrt{(\ell + \alpha)^2 + \beta^2} = \ell^2 - \alpha^2 + |\ell^2 - \alpha^2| \geq 0.$$

Thus,

$$\begin{aligned} \ell^2 - \alpha^2 + \sqrt{(\ell - \alpha)^2 + \beta^2} \sqrt{(\ell + \alpha)^2 + \beta^2} + \beta^2 \\ > \ell^2 - \alpha^2 + \sqrt{(\ell - \alpha)^2} \sqrt{(\ell + \alpha)^2} + \beta^2 \geq \beta^2 > 0 \end{aligned}$$

which settles the argument for $g'(\ell) > 0$.

Since $g(0) = 0$ and g is one-to-one, the case $\delta = 0$ is settled. So, let $\delta \neq 0$.

First we reformulate g by expanding the fraction by $\sqrt{+} + \sqrt{-}$ where we use the abbreviations $\sqrt{\pm} := \sqrt{(\ell \pm \alpha)^2 + \beta^2}$:

$$\begin{aligned} g(\ell) &= \frac{\ell(\sqrt{+} + \sqrt{-})^2 - \alpha(\sqrt{+}^2 - \sqrt{-}^2)}{(\sqrt{+} + \sqrt{-})^2} = \ell - \alpha \frac{\sqrt{+}^2 - \sqrt{-}^2}{(\sqrt{+} + \sqrt{-})^2} \\ &= \ell \left(1 - \frac{4\alpha^2}{(\sqrt{+} + \sqrt{-})^2} \right) = \ell \left(1 - \frac{2\alpha^2}{\ell^2 + \alpha^2 + \beta^2 + \sqrt{+}\sqrt{-}} \right) \\ &= \ell \frac{\ell^2 - \alpha^2 + \beta^2 + \sqrt{+}\sqrt{-}}{\ell^2 + \alpha^2 + \beta^2 + \sqrt{+}\sqrt{-}}. \end{aligned}$$

Thus, $g(\ell) = \delta$ if and only if

$$\ell(\ell^2 - \alpha^2 + \beta^2 + \sqrt{+}\sqrt{-}) = \delta(\ell^2 + \alpha^2 + \beta^2 + \sqrt{+}\sqrt{-}).$$

The latter equation is equivalent to

$$\ell(\ell^2 - \alpha^2 + \beta^2) - \delta(\ell^2 + \alpha^2 + \beta^2) = (\delta - \ell)\sqrt{+}\sqrt{-}.$$

Squaring both sides (caution: now we introduce multiple solutions) and doing a little algebra yield

$$-4\alpha^2 \ell (\delta \ell^2 + (\beta^2 - \delta^2) \ell - (\alpha^2 + \beta^2) \delta) = 0.$$

As $\alpha \neq 0$ and $\ell \neq 0$ (since $\delta \neq 0$) above equation has the two solutions for ℓ

$$\frac{\delta^2 - \beta^2 \pm \sqrt{(\delta^2 - \beta^2)^2 + 4\delta^2(\alpha^2 + \beta^2)}}{2\delta} = \frac{\delta^2 - \beta^2 \pm \sqrt{(\delta^2 + \beta^2)^2 + 4\delta^2\alpha^2}}{2\delta}.$$

From the asymptotics

$$\lim_{\ell \rightarrow -\infty} \frac{g(\ell)}{\ell} = 1 \quad \text{as well as} \quad \lim_{\ell \rightarrow \infty} \frac{g(\ell)}{\ell} = 1$$

we infer that the only solution of $g(\ell) = \delta \neq 0$ is

$$\ell = \frac{\delta^2 - \beta^2 + \sqrt{(\delta^2 + \beta^2)^2 + 4\delta^2\alpha^2}}{2\delta}$$

which is (5.8). Hence Lemma 3.4 is validated.

The proof of Lemma 3.6 is essentially the same but simpler. With $\ell := x_1 - s$ let

$$D := \sqrt{(\ell - \alpha)^2 + x_2^2} \quad \text{and} \quad E := \sqrt{(\ell + \alpha)^2 + x_2^2}.$$

Now, the two components of (3.8) read as

$$\xi_1 = \omega \left(\frac{\ell - \alpha}{D} + \frac{\ell + \alpha}{E} \right) \quad \text{and} \quad \xi_2 = \omega x_2 \left(\frac{1}{D} + \frac{1}{E} \right).$$

The latter equation yields that

$$(5.10) \quad \omega = \frac{\xi_2}{x_2 \left(\frac{1}{D} + \frac{1}{E} \right)}$$

and from the former we then immediately obtain that

$$g(\ell) = q x_2, \quad q := \xi_1 / \xi_2,$$

where g is as in (5.7) with β replaced by x_2 . Thus, $s = x_1 - g^{-1}(q x_2)$ is explicitly given by

$$(5.11) \quad s = \begin{cases} x_1 - \frac{1}{2q} \left((q^2 - 1)x_2 + \sqrt{(q^2 + 1)^2 x_2^2 + 4\alpha^2 q^2} \right) & : \xi_1 \neq 0, \\ x_1 & : \xi_1 = 0. \end{cases}$$

Now, we can express ω exclusively by \mathbf{x} and ξ which yields Lemma 3.6.

5.2. The symbol calculation and proof of Theorem 3.5. Since the symbol of $K F_3^\dagger \psi F_3$ is the symbol of the Ψ DO K multiplied by the symbol of $F_3^\dagger \psi F_3$ (and similarly for $K F_3^* \psi F_3$), we will calculate the symbols of $F_3^\dagger \psi F_3$ and of $F_3^* \psi F_3$.

Our method to calculate symbols is versatile, and it can be used for nonconstant sound speed in some cases and for arbitrary weights and a large range of other Radon transforms. We will sketch the important steps in the proof, referring to the original references for details. We follow the general calculation in [26] and refer to [20, 38] for details about FIOs (see also [22] for an overview).

We use the definition of Radon transform in [16, 17], and to do this, we put our transform in the framework of the double fibration. This framework was used by Helgason [18, 19] to define Radon transforms in a group setting, and it was generalized to manifolds without a group structure [12, 13] (see also, [17, p. 340-341, 370] [26, Sect. 1]). The double fibration defines sets of integration for the Radon transform in broad generality. Let X and Y be manifolds and let Z be a submanifold of $Y \times X$. We assume that the natural projections

$$(5.12) \quad \begin{array}{ccc} & Z & \\ \pi_Y \swarrow & & \searrow \pi_X \\ Y & & X \end{array}$$

are both fiber maps. In this case, we call (5.12) a *double fibration*. For $y \in Y$, the Radon transform integrates over the subset of X ,

$$E(y) = \pi_X (\pi_Y^{-1}(\{y\})) = \{x \in X \mid (y, x) \in Z\}.$$

Given smooth, positive measures μ on Z , m_X on X , and m_Y on Y , the measure for the integral transform on $E(y)$ is the quotient measure μ/m_Y (and μ/m_X for the dual transform). Since the maps π_X and π_Y are fiber maps, these quotient measure can be defined using local coordinates.

It is often assumed that π_X is a proper map. This means that the normal operator (for us $F_3^* F_3$) is defined for all compactly supported distributions. However, by including the cutoff ψ , we can compose F_3^* and ψF_3 without this assumption on π_X .

Recall that the L^2 adjoint of F_3 is F_3^* given in (3.2) with the same weight as F_3 :

$$(5.13) \quad F_3^* g(\mathbf{x}) = \int_Y A_3(\mathbf{s}, \mathbf{x}) g(\mathbf{s}, t) \delta(t - \varphi(\mathbf{s}, \mathbf{x})) d\mathbf{s} dt = \int_{S_0} A_3(\mathbf{s}, \mathbf{x}) g(\mathbf{s}, \varphi(\mathbf{s}, \mathbf{x})) d\mathbf{s}.$$

For our ellipsoidal transform, we let

$$(5.14) \quad Z = \{(\mathbf{s}, t, \mathbf{x}) \mid t - \varphi(\mathbf{s}, \mathbf{x}) = 0\},$$

and note that the ellipsoid is given by

$$(5.15) \quad E(\mathbf{s}_0, t_0) = \{x \in \mathbb{R}_+^3 \mid (\mathbf{s}_0, t_0, \mathbf{x}) \in Z\}.$$

We define a smooth positive measure on Z

$$(5.16) \quad \mu = A_3(\mathbf{s}, \mathbf{x}) \mu_0 \quad \text{where} \quad \mu_0 = \delta(t - \varphi(\mathbf{s}, \mathbf{x})) d\mathbf{s} dt d\mathbf{x}.$$

For $f \in \mathcal{D}(Y \times X)$,

$$\int f \mu = \int f(\mathbf{s}, t, \mathbf{x}) A_3(\mathbf{s}, \mathbf{x}) \delta(t - \varphi(\mathbf{s}, \mathbf{x})) d\mathbf{s} dt d\mathbf{x}.$$

We choose smooth positive measures $m_X = d\mathbf{x}$ on X and $m_Y = d\mathbf{s} dt$ on Y . Then, F_3 and F_3^* are the standard generalized Radon transforms defined on X and Y from these measures, e.g., the measure for F_3 is $\mu/(d\mathbf{s} dt)$ and the measure for F_3^* is $\mu/d\mathbf{x}$ (see (3.2)) and note that the weight for F_3^* is the same as for F_3 .

The Schwartz kernel of our Radon transform F_3 is integration over Z in smooth measure μ (see, e.g., [26, Proposition 1.1]). Note that the Schwartz kernel of F_3^* is integration over Z in measure μ and the Schwartz kernel of F_3^\dagger is integration with respect to the measure $W(\mathbf{s}, t, \mathbf{x}) \mu_0$.

Let \mathcal{C} be the canonical relation of F_3 , then

$$(5.17) \quad \mathcal{C} = \{(\mathbf{s}, \varphi(\mathbf{s}, \mathbf{x}), \omega \partial_{\mathbf{s}} \varphi - \omega dt, \mathbf{x}, \omega \partial_{\mathbf{x}} \varphi) \mid \mathbf{s} \in S_0, \mathbf{x} \in \mathbb{R}_+^3, \omega \neq 0\}$$

where $\partial_{\mathbf{x}} \varphi = \nabla_{\mathbf{x}} \varphi d\mathbf{x}$ is the partial differential in \mathbf{x} , etc. Let $\Pi_Y: \mathcal{C} \rightarrow T^*(Y) \setminus \{\mathbf{0}\}$ and $\Pi_X: \mathcal{C} \rightarrow T^*(X) \setminus \{\mathbf{0}\}$ be the natural projections. In [8], Felea et al. proved that the microlocal Bolker assumption holds:

$$(5.18) \quad \Pi_Y: \mathcal{C} \rightarrow T^*(Y) \setminus \{\mathbf{0}\} \quad \text{is an injective immersion.}$$

To use the calculations in [26], we introduce the new variable $w = t - \varphi(\mathbf{s}, \mathbf{x})$, and note that $\delta(w)$ corresponds to the Dirac delta in the definition of μ_0 . We let η be the differential dw and let $d\eta$ be the one form dual to η . So $d\eta(\frac{\partial}{\partial \eta}) = 1$.

Here we are viewing any measure on an n -dimensional manifold M as the absolute value of an associated alternating n -form in its cotangent space that evaluates on the n -fold wedge product $\wedge^n T(M)$. So, if $x \in M$ and v_1^*, \dots, v_n^* are covectors in $T_x^*(M)$ and u_1, \dots, u_n are vectors in $T_x(M)$ then the measure $|v_1^* \wedge \dots \wedge v_n^*|$ evaluated at (u_1, \dots, u_n) is

$$(5.19) \quad |v_1^* \wedge \dots \wedge v_n^*|(u_1 \wedge \dots \wedge u_n) = |\det(v_i^*(u_j)_{i=1, \dots, n, j=1, \dots, n})|$$

as defined in [39, p. 59].

By applying the arguments below (14) in [26], the symbol of F_3 as an FIO is

$$\frac{(2\pi)^{(3-1)/2} A_3 d\mathbf{x}}{\Pi_X(|\sigma_X|^{3/2})}$$

and the symbol of $F_3^*\psi$ as an FIO is

$$\frac{(2\pi)^{(3-1)/2} A_3 \psi \, ds \, dt}{\Pi_Y \left(|\sigma_Y|^{3/2} \right)}.$$

Since F_3 and \mathcal{C} satisfy the microlocal Bolker assumption, we can use Theorem 2.1 in [26] to see that

$$(5.20) \quad \sigma(F_3^* \psi F_3)(\mathbf{x}, \xi) = \frac{(2\pi)^{3-1} \psi(\mathbf{s}, t) \mu^2 d\omega d\eta}{m_X m_Y \Pi_X^* \left(|\sigma_X|^{3/2} \right) \Pi_Y^* \left(|\sigma_Y|^{3/2} \right)}$$

where $\mathbf{x} \in \mathbb{R}^3$, $\xi \in \mathbb{R}^3 \setminus \{\mathbf{0}\}$, σ_X is the symplectic two-form [20], $|\sigma_X|^3$ is the standard measure on $T^*(X)$, σ_Y is the symplectic two-form and $|\sigma_Y|^3$ is the standard measure on $T^*(Y)$ [20, p. 168]. One evaluates the symbol at all points

$$(\mathbf{x}', \xi' d\mathbf{x}, \mathbf{s}, t, \eta, \mathbf{s}, t, \eta, \mathbf{x}, \xi d\mathbf{x}) \in (\mathcal{C}^t \times \mathcal{C}) \cap (T^*(X) \times \Delta_Y \times T^*(X))$$

where Δ_Y denotes the diagonal in $T^*(Y)$. By the Bolker assumption, $(\mathbf{x}', \xi' d\mathbf{x}) = (\mathbf{x}, \xi d\mathbf{x})$, so this set can be identified with the inverse image of $(\mathbf{x}, \xi d\mathbf{x})$ under $\Pi_X : \mathcal{C} \rightarrow T^*(X)$. Using Lemma 3.4 and the expression (5.17), one sees that Π_X is injective. Therefore, this inverse image is the single point given by the projection $\Pi_X(\lambda) = (\mathbf{x}, \xi d\mathbf{x})$ where $\xi = \omega \nabla_{\mathbf{x}} \varphi$ by (5.17).

Using the definition of the measures m_X , m_Y and μ , the symbol simplifies to

$$(5.21) \quad \sigma(F_3^* \psi F_3)(\mathbf{x}, \xi) = \frac{(2\pi)^2 A_3^2(\mathbf{s}, \mathbf{x}) \psi(\mathbf{s}, \mathbf{x}) \, d\mathbf{x} \, ds \, d\eta}{\Pi_X^* \left(|\sigma_X|^{3/2} \right) \Pi_Y^* \left(|\sigma_Y|^{3/2} \right)}$$

evaluated at this preimage $\lambda = \Pi_X^{-1}(\mathbf{x}, \xi d\mathbf{x})$ in \mathcal{C} .

The following lemma finishes the proof for $F_3^* \psi F_3$.

Lemma 5.1. *We have that*

$$(5.22) \quad \frac{d\mathbf{x} \, ds \, d\eta}{\Pi_X^* \left(|\sigma_X|^{3/2} \right) \Pi_Y^* \left(|\sigma_Y|^{3/2} \right)} = \frac{1}{|\omega|^2 B_3(\mathbf{s}, \mathbf{x})}$$

evaluated at $\Pi_X^{-1}(\mathbf{x}, \xi d\mathbf{x})$ and where B_3 is given by (3.6) and $\mathbf{s} = \mathbf{s}(\mathbf{x}, \xi)$ is given by (5.5), and (5.9).

Proof. The lemma is proved by first calculating a basis of $T(\mathcal{C})$ using the coordinates $(\mathbf{s}, \mathbf{x}, \omega)$. This gives a basis \mathcal{B} of the wedge product $\wedge^6 T(\mathcal{C})$. One evaluates the measure $d\mathbf{x} \, ds \, d\eta$ on \mathcal{B} using (5.19). One then evaluates $\Pi_X^* \left(|\sigma_X|^{3/2} \right)$ by evaluating $|\sigma_X|^{3/2}$ on the push forward $\Pi_{X*}(\mathcal{B})$ and one evaluates $\Pi_Y^* \left(|\sigma_Y|^{3/2} \right)$ in a similar way. By comparing the results, one shows (5.22). \square

The proof for $F_3^\dagger \psi F_3$ is similar but one uses the measure $W\mu_0$ on Z (where μ_0 is given by (5.16)) to define F_3^\dagger as a Radon transform.

The proof of the theorem for \mathbb{R}^2 is essentially the same except that $\mathbf{s} \in \mathbb{R}^2$ is replaced by the single coordinate $s \in \mathbb{R}$ and the coordinates we use on \mathcal{C} are (s, \mathbf{x}, ω) .

REFERENCES

- [1] G. Beylkin. Imaging of discontinuities in the inverse scattering problem by inversion of a causal generalized Radon transform. *J. Math. Phys.*, 26(1):99–108, 1985.
- [2] N. Bleistein, J. Cohen, and J. J.W. Stockwell. *Mathematics of Multidimensional Seismic Imaging, Migration, and Inversion*, volume 13 of *Interdisciplinary Applied Mathematics*. Springer, New York, 2001.
- [3] V. Brytik, M. V. de Hoop, and R. D. van der Hilst. Elastic-wave inverse scattering based on reverse time migration with active and passive source reflection data. In *Inverse problems and applications: inside out. II*, volume 60 of *Math. Sci. Res. Inst. Publ.*, pages 411–453. Cambridge Univ. Press, Cambridge, 2013.
- [4] J. K. Cohen and N. Bleistein. Velocity inversion procedure for acoustic waves. *Geophysics*, 44(6):1077–1085, 1979.
- [5] R. Courant and D. Hilbert. *Methods of mathematical physics. Vol. II*. Wiley Classics Library. John Wiley & Sons Inc., New York, 1989. Partial differential equations, Reprint of the 1962 original, A Wiley-Interscience Publication.
- [6] M. V. de Hoop, H. Smith, G. Uhlmann, and R. D. van der Hilst. Seismic imaging with the generalized Radon transform: a curvelet transform perspective. *Inverse Problems*, 25(2):025005, 21, 2009.
- [7] R. Felea and A. Greenleaf. Fourier integral operators with open umbrellas and seismic inversion for cusp caustics. *Math. Res. Lett.*, 17(5):867–886, 2010.
- [8] R. Felea, V. P. Krishnan, C. J. Nolan, and E. T. Quinto. Common midpoint versus common offset acquisition geometry in seismic imaging. *Inverse Probl. Imaging*, 10(1):87–102, 2016.
- [9] F. G. Friedlander. *Introduction to the theory of distributions*. Cambridge University Press, Cambridge, second edition, 1998. With additional material by M. Joshi.
- [10] J. Frikel and E. T. Quinto. Artifacts in incomplete data tomography with applications to photoacoustic tomography and sonar. *SIAM J. Appl. Math.*, 75(2):703–725, 2015.
- [11] J. Frikel and E. T. Quinto. Limited data problems for the generalized Radon transform in \mathbb{R}^n . *SIAM J. Math. Anal.*, 48:2301–2318, 2016.
- [12] I. M. Gelfand and M. I. Graev. Geometry of homogeneous spaces, representations of groups in homogeneous spaces and related questions of integral geometry. *Trudy Moskov. Mat. Obshch.*, 8:321–390, 1959.
- [13] I. M. Gelfand, M. I. Graev, and Z. Y. Shapiro. Differential forms and integral geometry. *Functional Anal. and Appl.*, 3:24–40, 1969.
- [14] C. Grathwohl, P. Kunstmann, E. T. Quinto, and A. Rieder. Approximate inverse for the common offset acquisition geometry in 2D seismic imaging. *Inverse Problems*, 34(1):014002, 2018. <https://doi.org/10.1088/1361-6420/aa9900>.
- [15] A. Greenleaf and G. Uhlmann. Non-local inversion formulas for the X-ray transform. *Duke Math. J.*, 58:205–240, 1989.
- [16] V. Guillemin. Some remarks on integral geometry. Technical report, MIT, 1975.
- [17] V. Guillemin and S. Sternberg. *Geometric Asymptotics*. American Mathematical Society, Providence, RI, 1977.
- [18] S. Helgason. Differential operators on homogeneous spaces. *Acta Math.*, 102:239–329, 1959.
- [19] S. Helgason. A duality in integral geometry on symmetric spaces. In *Proc. U.S.-Japan Seminar in Differential Geometry, Kyoto, 1965*, pages 37–56, Tokyo, 1966. Nippon Hyonsha.
- [20] L. Hörmander. Fourier Integral Operators, I. *Acta Mathematica*, 127:79–183, 1971.
- [21] V. P. Krishnan, H. Levinson, and E. T. Quinto. Microlocal analysis of elliptical Radon transforms with foci on a line. In I. Sabadini and D. Struppa, editors, *The Mathematical Legacy of Leon Ehrenpreis, 1930-2010*, volume 16 of *Springer Proceedings in Mathematics*, pages 163–182. Springer, 2012.
- [22] V. P. Krishnan and E. T. Quinto. Microlocal Analysis in Tomography. In O. Scherzer, editor, *Handbook of Mathematical Methods in Imaging*, chapter 18, pages 847–902. Springer Verlag, New York, Berlin, 2015.
- [23] C. J. Nolan and M. Cheney. Microlocal analysis of synthetic aperture radar imaging. *J. Fourier Anal. Appl.*, 10(2):133–148, 2004.
- [24] C. J. Nolan and W. W. Symes. Global solution of a linearized inverse problem for the wave equation. *Comm. Partial Differential Equations*, 22(5-6):919–952, 1997.
- [25] B. Petersen. *Introduction to the Fourier Transform and Pseudo-Differential Operators*. Pitman, Boston, 1983.

- [26] E. T. Quinto. The dependence of the generalized Radon transform on defining measures. *Trans. Amer. Math. Soc.*, 257:331–346, 1980.
- [27] E. T. Quinto. Singularities of the X-ray transform and limited data tomography in \mathbb{R}^2 and \mathbb{R}^3 . *SIAM J. Math. Anal.*, 24(5):1215–1225, 1993.
- [28] E. T. Quinto, A. Rieder, and T. Schuster. Local inversion of the sonar transform regularized by the approximate inverse. *Inverse Problems*, 27(3):035006, Feb. 2011.
- [29] Rakesh. A linearised inverse problem for the wave equation. *Comm. Partial Differential Equations*, 13(5):573–601, 1988.
- [30] R. E. Sheriff. *Encyclopedic Dictionary of Applied Geophysics*. Society Of Exploration Geophysicists, Tulsa, OK, USA, 2002.
- [31] P. Stefanov, G. Uhlmann, and A. Vasy. Local recovery of the compressional and shear speeds from the hyperbolic DN map. *Inverse Problems*, 34:014003, 2018.
- [32] C. C. Stolk. Microlocal analysis of a seismic linearized inverse problem. *Wave Motion*, 32(3):267–290, 2000.
- [33] C. C. Stolk and M. V. de Hoop. Microlocal analysis of seismic inverse scattering in anisotropic elastic media. *Comm. Pure Appl. Math.*, 55(3):261–301, 2002.
- [34] C. C. Stolk and M. V. de Hoop. Seismic inverse scattering in the downward continuation approach. *Wave Motion*, 43(7):579–598, 2006.
- [35] W. W. Symes. Mathematics of reflection seismology. Technical report, The Rice Inversion Project, Rice University, Houston, TX, USA, 1998. <http://www.trip.caam.rice.edu/downloads/preamble.pdf>.
- [36] A. P. E. ten Kroode and D.-J. Smit. A microlocal analysis of a linearized inversion problem. In *Inverse problems in geophysical applications (Yosemite, CA, 1995)*, pages 146–162. SIAM, Philadelphia, PA, 1997.
- [37] A. P. E. ten Kroode, D.-J. Smit, and A. R. Verdel. A microlocal analysis of migration. *Wave Motion*, 28(2):149–172, 1998.
- [38] F. Trèves. *Introduction to Pseudodifferential and Fourier Integral Operators*. Volume 2: Fourier Integral Operators. Plenum Press, New York and London, 1980.
- [39] F. Warner. *Foundations of Differential Manifolds and Lie Groups*. Scott Foreman and Co., Glenview, IL, USA, 1970.

DEPARTMENT OF MATHEMATICS, KARLSRUHE INSTITUTE OF TECHNOLOGY (KIT), D-76128 KARLSRUHE, GERMANY

E-mail address: `christine.grathwohl@kit.edu`

E-mail address: `peer.kunstmann@kit.edu`

E-mail address: `andreas.rieder@kit.edu`

DEPARTMENT OF MATHEMATICS, TUFTS UNIVERSITY, MEDFORD, MA 02155, USA

E-mail address: `todd.quinto@tufts.edu`